

## **A Giant Planet Around a Metal-poor Star of Extragalactic Origin**

Johny Setiawan<sup>1</sup>, Rainer J. Klement<sup>1</sup>, Thomas Henning<sup>1</sup>, Hans-Walter Rix<sup>1</sup>,  
Boyke Rochau<sup>1</sup>, Jens Rodmann<sup>2</sup>, Tim Schulze-Hartung<sup>1</sup>

Received \_\_\_\_\_; accepted \_\_\_\_\_

---

<sup>1</sup>Max-Planck-Institut für Astronomie, Königstuhl 17, D-69117 Heidelberg; setiawan@mpia.de

<sup>2</sup>European Space Agency, Space Environment and Effects Section, ESTEC, Keplerlaan 1, 2201  
AZ Noordwijk, The Netherlands

## 1. Main text

In the last two decades, several hundred planets have been detected beyond our Solar-system. Most of these extra-solar planets orbit sun-like stars. A small number have been detected around stars that are in their late evolutionary state, such as Red Giant Branch (RGB) stars and pulsars. The phase directly after the RGB stage, the Horizontal Branch (HB), however, is still unexplored; therefore, there is no empirical evidence for whether close-in planets, i.e., those with semi-major axes less than 0.1 AU, survive the giant phase of their host stars.

Besides its evolutionary stage, a star's chemical composition appears to be a major indicator of its probability for hosting a planet. Previous studies, e.g., Gonzales (1997), showed that main-sequence (MS) stars that host giant planets are metal-rich. This finding is supported by the large exoplanet search surveys around MS stars reporting a connection between planet frequency and metallicity (Santos et al. 2004; Valenti & Fischer 2005), and a survey of 160 metal-poor main-sequence stars finding no evidence for Jovian planets (Sozzetti et al. 2009).

Until now, only very few planets have been detected around stars with metallicities as low as  $[\text{Fe}/\text{H}] = -1$ , i.e. 10% of the sun's metallicity. The detection of PSR B1620 b, a Jovian planet orbiting a pulsar in the core of the metal-poor globular cluster M4 ( $[\text{Fe}/\text{H}] = -1.2$ ), suggests, however, that planets may form around metal-poor stars (Ford et al. 2000; Sigurdsson et al. 2003), although the formation mechanism of this particular planet might be linked to the dense cluster environment (Beer et al. 2004).

We used the Fibre-fed Extended Range Optical Spectrograph (FEROS), a high-resolution spectrograph ( $R = 48,000$ ) attached to the 2.2 meter Max-Planck Gesellschaft/European Southern Observatory (MPG/ESO) telescope<sup>1</sup>, to observe the star HIP 13044. This star is classified as

---

<sup>1</sup>The observations of HIP 13044 were carried out from September 2009 until July 2010. The

a red HB (RHB) star (Fig. 1) and its metal content is  $[\text{Fe}/\text{H}]_{\text{mean}} = -2.09$  (Beers et al. 1990; Chiba & Beers 2000; Carney et al. 2008b; Roederer et al. 2010), i.e. about 1% that of the Sun. So far, HIP 13044 is not known as a binary system. Detailed stellar parameters can be found in Supporting Online Material, Section 2.1.

Previous radial velocity (RV) measurements of HIP 13044 showed a systematic velocity of about  $300 \text{ km s}^{-1}$  with respect to the Sun, indicating that the star belongs to the stellar halo (Carney et al. 1986). Indeed, the star has been connected to the Helmi stream (Helmi et al. 1999), a group of stars that share similar orbital parameters that stand apart from those of the bulk of other stars in the solar neighborhood. The Helmi stream stars move on prograde eccentric orbits ( $R_{\text{peri}} \sim 7 \text{ kpc}$ ,  $R_{\text{apo}} \sim 16 \text{ kpc}$ ) that reach distances up to  $|z|_{\text{max}} \sim 13 \text{ kpc}$  above and below the galactic plane. From that, it has been concluded that these stars were once bound to a satellite galaxy of the Milky Way (Helmi et al. 1999; Chiba & Beers 2000) that was tidally disrupted 6–9 Ga ago (Kepley et al. 2007).

The variation of the RV between our observations at different epochs has a semi-amplitude of  $120 \text{ m s}^{-1}$  (Fig. 2). The Generalized Lomb Scargle (GLS) periodogram (Zechmeister & Kürster 2009) reveals a significant RV periodicity at  $P = 16.2$  days with a False Alarm Probability of  $5.5 \times 10^{-6}$ . Additional analysis, using a Bayesian algorithm (Gregory 2005), yields a similar period around 16 days. Such RV variation can be induced by an unseen orbiting companion,

---

spectrograph covers a wavelength range from 350 to 920 nm (Kaufer et al. 2000). To measure the RV values of HIP 13044 we used a cross-correlation technique, where the stellar spectrum is cross-correlated with a numerical template (mask) designed for stars of the spectral type F0 (Section 2.2).

<sup>2</sup>In order to search for periodic variations, we used periodogram analysis techniques, which are capable of treating missing values and unevenly spaced time points.

by moving/rotating surface inhomogeneities or by non-radial stellar pulsations. Exploring both stellar rotational modulation and pulsations is critical when probing the presence of a planetary companion, because they can produce a similar or even the same RV variation, mimicking a Keplerian motion.

A well-established technique to detect stellar rotational modulation is to investigate the line profile asymmetry or bisector (Gray et al. 2008) and Ca II lines (Section 2.3). Surface inhomogeneities, such as starspots and large granulation cells, produce asymmetry in the spectral line profiles. When a spotted star rotates, the barycenter of the line profiles moves periodically and the variation can mimic a RV variation caused by an orbiting companion. Instead of measuring the bisectors, one can equivalently use the bisector velocity spans (BVS) to search for rotational modulation (Hatzes 1996). Adopting this technique, we have measured BVS from the stellar spectra. There is only a weak correlation between BVS and RV (correlation coefficient =  $-0.13$ ), but the BVS variation shows a clear periodicity with  $P = 5.02$  days (Section 2.3.1). No period around 16 days is found in the BVS variation.

In addition to the BVS analysis, we investigated the variation of the Ca II  $\lambda 849.8$  line, which is one of the Ca II infrared triplet lines. From the observed Ca II 849.8 equivalent-width variations we computed a mean period of 6.05 days (Section 2.3.1), which is in the same order of the period of the BVS variation. We adopted the mean period of both stellar activity indicators,  $P_{\text{rot}} = 5.53 \pm 0.73$  days, as the stellar rotation period of HIP 13044 and then calculated the inclination angle of the stellar rotation axis, which follows from  $P_{\text{rot}} / \sin i = 2\pi R_* / v \sin i$ . With a stellar radius  $R_* = 6.7 R_{\odot}$  Carney et al. (2008a) and our adopted value for the projected rotational velocity,  $v \sin i = 10.25 \text{ km s}^{-1}$ , which was derived from the observed line broadening (Section 2.1), we obtained an inclination angle  $i = 9.7 \pm 1.3$  deg. Thus, the real stellar rotation velocity is  $\sim 62 \text{ km s}^{-1}$ , which is typical for an early F type MS-star but relatively high for HB stars.

An explanation for this high rotation velocity is the assumption that HIP 13044 has engulfed its close-in planets during the red giant phase. Infalling planets are able to spin-up their host star (Soker 1998; Levrard et al. 2009; Carlberg et al. 2009), and this mechanism has been suggested to explain the high  $v \sin i$  values observed for many RGB and HB stars (Carney et al. 2003).

We observed variations of HIP 13044 in the photometric data from the Hipparcos satellite (Perryman et al. 1997) and SuperWASP (Pollacco et al. 2006) (Section 2.3.2). While the Hipparcos data shows only a marginal significant periodicity of 7.1 hours (FAP=1.8%), the SuperWASP data shows few intra-day periodicities with FAP $\sim$ 1% and two significant periodicities at 1.39 (FAP= $5 \times 10^{-4}$ ) and 3.53 days (FAP= $2 \times 10^{-4}$ ). These two periods, however, are most likely harmonic to each other ( $1.4^{-1} + 3.5^{-1} = 1$ ). It is expected that HIP 13044 oscillates only at pulsationally unstable overtones of high order (Xiong et al. 1998). Observations of one RHB star in the metal-poor globular cluster NGC 6397 (Stello & Gilliland 2009) as well as theoretical predictions (Xiong et al. 1998) set these periods in the range of a few hours to a day or so. No clear theoretical predictions for a star with parameters similar to HIP 13044 exist, hence it is possible that some high-order oscillations are able to explain the 1.4 or 3.5 day signal. What is important, however, is that there is no signal of a period around 16.2 d in the photometric data.

The arguments above show that neither stellar rotational modulation nor pulsations are plausible sources of the observed periodic RV variation. Therefore, the best explanation for the  $\sim$ 16 days period is the presence of an unseen companion. We computed its orbital solution (Table 1). Its minimum mass lies securely in the planetary mass domain, even with a plausible  $\sin i$  uncertainty. With an eccentricity of 0.25 and a semi-major axis of 0.116 AU, the planet has a periastron distance of about 0.087 AU which is  $\approx$ 2.8 times the present stellar radius. The periastron is  $\sim$ 0.06 AU away from the stellar surface.

Because a large number of known exoplanets have orbital semi-major axes between 0.01 and

Table 1: Orbital parameters of HIP 13044 b

$P$	$16.2 \pm 0.3$	days
$K_1$	$119.9 \pm 9.8$	$\text{m s}^{-1}$
$e$	$0.25 \pm 0.05$	
$\omega$	$219.8 \pm 1.8$	deg
$JD_0 - 2450000$	$5109.78 \pm 0.02$	days
$\chi^2$	32.35	$\text{m s}^{-1}$
$rms$	50.86	$\text{m s}^{-1}$
$m_2 \sin i$	$1.25 \pm 0.05$	$M_{\text{Jup}}$
$a$	$0.116 \pm 0.01$	AU

0.06 AU, the distance between the periastron and the star HIP 13044 itself is not unusual. The non-circular orbit ( $e = 0.25$ ), however, is not expected for a close-in giant planet around a post RGB star.

In the case of HIP 13044, the original orbit could have been disturbed or changed during the evolution of the star-planet-system, in particular during the RGB phase (Soker 1998). Interestingly, the orbital period of HIP 13044 b is close to three times the stellar rotation period. There are a number of known planetary systems which also have such a “coupling” between the stellar rotation and orbital periods, e.g. Tau Boo (1:1), HD 168433 (1:2), HD 90156 (1:2) and HD 93083 (1:3). Such planetary systems are particularly interesting to study star-planet interactions (Shkolnik et al. 2008).

So far, there are only very few planet or brown dwarf detections around post RGB stars besides the pulsar planets, namely V391 Peg (Silvotti et al. 2007), HW Vir (Lee et al. 2009) and HD 149382 (Geier et al. 2009) (Fig. 1). These are, however, substellar companions around

subdwarf-B or Extreme Horizontal Branch (EHB) stars, i.e., the nature of their host stars differs from that of HIP 13044, an RHB star. Contrary to RGB stars, such as G and K giants (Walker et al. 1992; Hatzes & Cochran 1993; Setiawan et al. 2004; Döllinger et al. 2007) and subgiants (e.g. Johnson et al. 2010), HB stars have not been yet extensively surveyed for planets.

While at least 150 main-sequence stars are known to bear close-in ( $a = 0.1$  AU) giant planets, so far no such planets have been reported around RGB stars. A possible explanation is that the inner planets have been engulfed by the star when the stellar atmosphere expanded during the giant phase. The survival of HIP 13044 b during that phase is theoretically possible under certain circumstances (Livio & Soker 1983; Soker 1998; Bear & Soker 2010). It is also possible that the planet's orbit decayed through tidal interaction with the stellar envelope. However, a prerequisite to survival is then that the mass loss of the star stops before the planet would have been evaporated or accreted. Assuming asymmetric mass loss, velocity kicks could have increased the eccentricity of HIP 13044 b to its current, somewhat high value (Heyl 2007). The same could be achieved by interaction with a third body in the system.

Interestingly, a survey to characterize the multiplicity of EHB stars showed that more than 60% of the sample are close binaries (Maxted et al. 2001). Their orbital radii are much smaller than the stellar radius in the RGB phase. This could be explained by the high friction in the interstellar medium, which would move a distant companion towards the primary. Such spiral-in mechanism could also take place in the RGB-to-RHB transition phase. Similar to the binary case, a distant giant planet in the RGB phase can move towards the primary into a smaller orbit. Consequently, the resulting close orbiting planets will be engulfed when the stellar envelope expands again in the next giant phase. HIP 13044 b could be a planet that is just about to be engulfed by its star.

HIP 13044, with a mean metallicity estimate of  $[\text{Fe}/\text{H}]=-2.1$ , is far more metal-poor than

any previously known exoplanet hosting star (Fig. 3). For the existing theories of hot giant planet formation, metallicity is an important parameter: in particular, it is fundamental for the core-accretion planet formation model (Ida & Lin 2005). It might be that initially, in the planet formation phase, HIP 13044 had a higher metallicity, and that during its subsequent evolution, it lost its heavier elements. For example, during the giant phase, heavy elements could have had been incorporated into dust grains and then separated from the star’s atmosphere (Mathis & Lamers 1992). However, given the star’s membership to the Helmi stream, in which the most metal-rich sub-dwarfs known so far have  $[\text{Fe}/\text{H}] \sim -1.5$  (Klement et al. 2009), we do not expect its initial Fe abundance to exceed this value.

Finally, as a member of the Helmi stream, HIP 13044 most probably has an extragalactic origin. This implies that its history is likely different from those of the majority of known planet-hosting stars. HIP 13044 was probably attracted to the Milky Way several Ga ago. Before that, it could have had belonged to a satellite galaxy of the Milky Way similar to Fornax or the Sagittarius dwarf spheroidal galaxy (Helmi et al. 1999). Because of the long galactic relaxation timescale, it is extremely unlikely that HIP 13044 b joined its host star through exchange with some Milky Way star, after the former had been tidally stripped. The planet HIP 13044 b could thus have a non-Galactic origin.

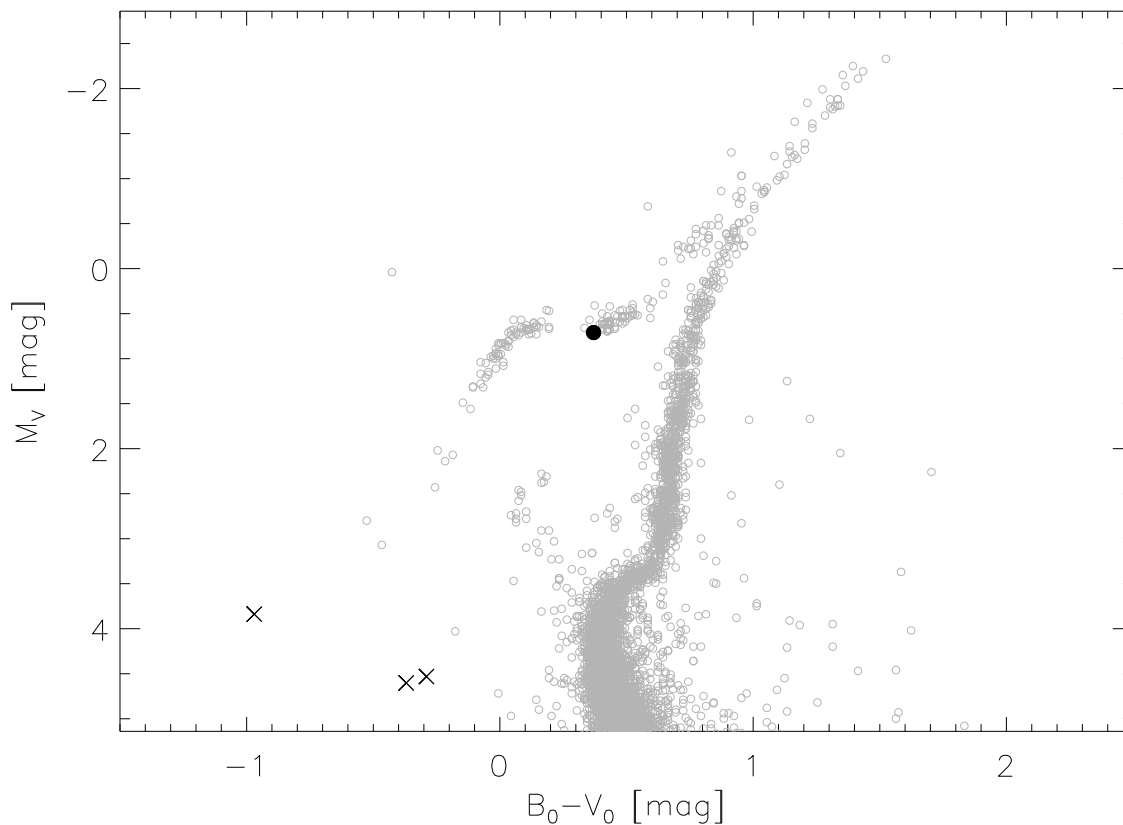


Fig. 1.— Location of HIP 13044 in a  $M_V$  vs.  $B - V$  color-magnitude diagram (CMD) shown as a black dot superimposed to the CMD of Messier 3 (grey open circles) based on the photometry by Buonanno et al. (1994). Apparent magnitudes have been converted to absolute magnitudes by considering the distance modulus and extinction given by Harris (1996). The gap separating the blue and red Horizontal Branch (HB) is due to RR Lyrae instability strip. The CMD location of HIP 13044 implies that it is a core He-burning star, located at the blue edge of the RHB. Further candidates for post RGB stars hosting planets/brown dwarf, V391 Peg, HW Vir and HD 149382 (Silvotti et al. 2007; Lee et al. 2009; Geier et al. 2009) are displayed as crosses.

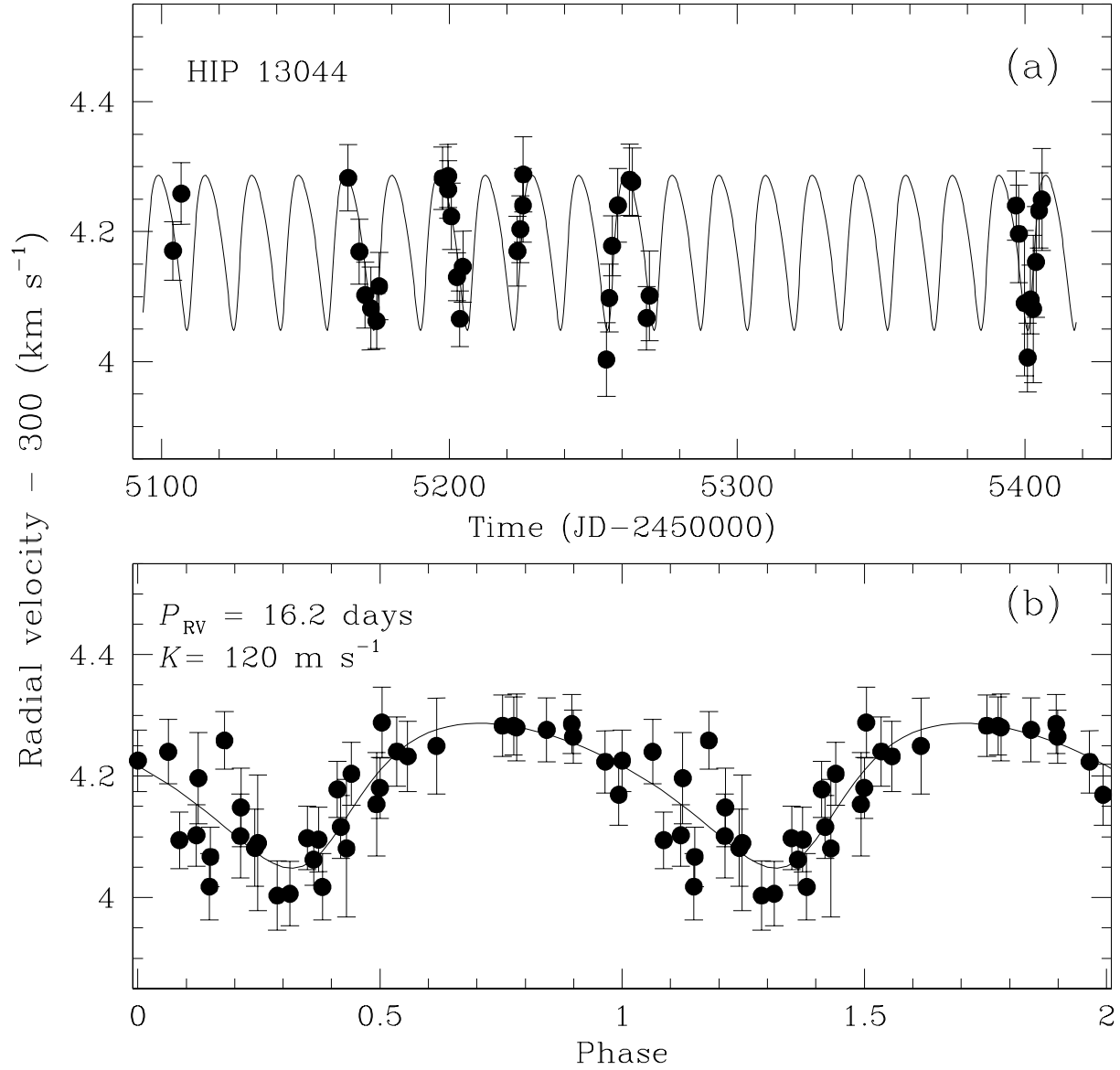


Fig. 2.— (Upper panel) RV variation of HIP 13044. The RV values have been computed from the mean RVs of 20 usable echelle orders of the individual spectrum. The error bars have been calculated from the standard error of the mean RV of each order. (Lower panel) RV variation phase-folded with  $P = 16.2$  days.

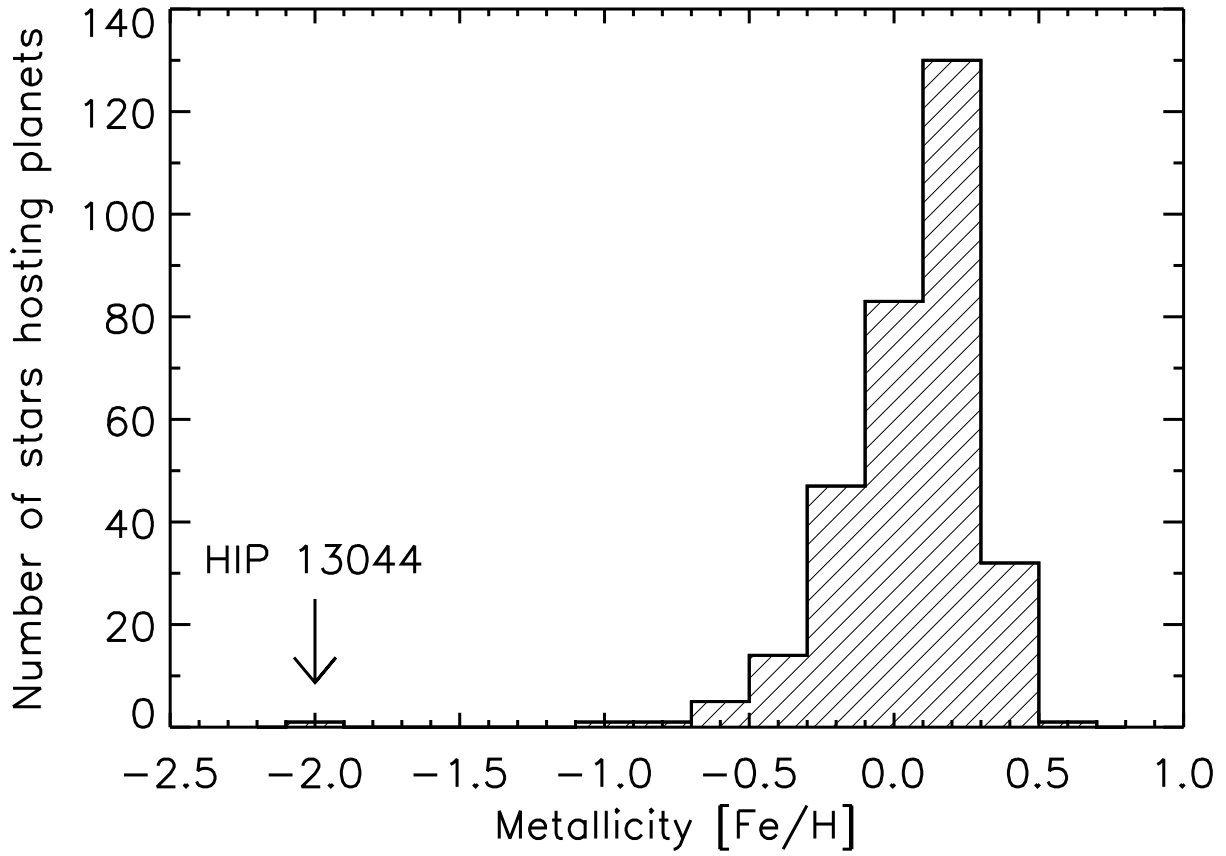


Fig. 3.— Distribution of the metallicity [Fe/H] of planet-hosting stars.

## 2. Supporting online material

This supplementary online material is part of the article with the title **”A Giant Planet Around a Metal-poor Star of Extragalactic Origin”**. Here we give additional information about the stellar parameters of HIP 13044 (Section 2.1) and more detailed descriptions of the observations as well as the stellar radial velocity (RV) computations (Section 2.2). As reported in the manuscript, the RV variation has a period of 16.2 days and semi-amplitude of  $120 \text{ m s}^{-1}$  which most likely originate from an unseen planetary companion. In the following sections we describe briefly the technique that we used to investigate the stellar activity (Section 2.3). We analyzed the line profile asymmetry (bisector) and Ca II  $\lambda 849.8$  line, which are excellent stellar activity indicators. Additionally, we also present our analysis of the Hipparcos and SuperWASP photometric data.

### 2.1. Stellar parameters

HIP 13044 (CD-36 1052, CPD-36 287) is a star of spectral type F2 (SIMBAD). It has a visual magnitude of  $m_V = 9.94$  mag (Hipparcos) and distance of  $\sim 700$  pc (Carney et al. 1986, 2008a). HIP 13044 resides in the red part of the Horizontal Branch (RHB), which is separated from the blue and extreme Horizontal Branch (BHB and EHB) stars by the RR Lyrae instability strip.

The Hipparcos archive data (Perryman et al. 1997) revealed variations in the photometry and astrometry. From the Hipparcos intermediate astrometry data, we calculated the *rms* of the difference between the observed great-circle abscissa and the solution computed with the reference astrometric parameters to be  $9 \times 10^{-3}$  arcsec. While the Hipparcos photometry data shows only a marginal significant periodicity at  $P = 7.1$  hours, photometric observations with SuperWASP (Pollacco et al. 2006) reveal some periodicities with timescales of several hours up to few days (Section 2.3.2). These signals might correspond to the stellar pulsations.

As a member of the Helmi stellar stream (Helmi et al. 1999), HIP 13044 shares the property of other stream members, like the low iron abundances ( $[\text{Fe}/\text{H}] = -1.8$  for 33 stream members) (Kepley et al. 2007; Klement et al. 2009) and a chemical similarity to typical inner halo stars (Roederer et al. 2010). An extensive abundance analysis of HIP 13044 has been also presented in Roederer et al. (2010).

Table. S1

Stellar parameters of HIP 13044

Parameter	Value	Unit	Reference
Spectral type	F2		SIMBAD
$m_V$	9.94	mag	Hipparcos
distance	$701 \pm 20$	pc	Beers et al. (1990); Carney et al. (1986, 2008a)
$T_{\text{eff}}$	$6025 \pm 63$	K	Carney et al. (2008a); Roederer et al. (2010)
$R_*$	$6.7 \pm 0.3$	$R_\odot$	Carney et al. (2008a)
$\log g$	$2.69 \pm 0.3$		Carney et al. (2008a)
$m$	$0.8 \pm 0.1$	$M_\odot$	this work
$[Fe/H]$	$-2.09 \pm 0.26$	$[\text{Fe}/\text{H}]_\odot$	Chiba & Beers (2000); Carney et al. (2008b); Roederer et al. (2010); Beers et al.
$v \sin i$	$8.8 \pm 0.8$	$\text{km s}^{-1}$	Carney et al. (2008a)
	$11.7 \pm 1.0$	$\text{km s}^{-1}$	this work

Table S1 summarizes the fundamental stellar parameters, such as the effective temperature  $T_{\text{eff}}$ , surface gravity  $\log g$ , stellar radius  $R_*$ , stellar mass and metallicity  $[\text{Fe}/\text{H}]$ , from the literature and our spectroscopic measurements. The stellar mass has been inferred from the knowledge of the stellar radius  $R_*$  and surface gravity  $\log g$ . We calculated a stellar mass of  $0.8 \pm 0.1 M_\odot$ . Carney et al. (2008a) have measured  $v \sin i = 8.8 \text{ km s}^{-1}$ , whereas we obtained  $v \sin i = 11.7 \text{ km s}^{-1}$ . The discrepancy between the two results is probably caused by the different methods used. Carney et al. (2008a) used a Fourier transform method, whereas we used a

cross-correlation technique to measure the  $v \sin i$  (Setiawan et al. 2004). For this work we adopt  $v \sin i = 10.25 \pm 2.1 \text{ km s}^{-1}$  which is the mean value of both measurements.

## 2.2. Radial velocity measurements

The observations of HIP 13044 have been performed with FEROS, a high-resolution spectrograph ( $R = 48\,000$ ) attached to the 2.2 meter MPG/ESO telescope, located at the ESO La Silla observatory. The spectrograph is equipped with two fibers and has a wavelength coverage from 350 to 920 nm that is divided into 39 echelle orders (Kaufer et al. 2000). The first fiber is used to record the stellar spectrum, whereas the second fiber can be used for a simultaneous calibration with a ThArNe lamp, in which the instrumental velocity drift during the night can be corrected.

The raw spectroscopic data have been reduced with an online data reduction pipeline that produced 39 one-dimensional spectra of each fiber. The stellar RVs have been computed by using a cross-correlation technique, where the stellar spectrum is cross-correlated with a numerical template (mask). The data reduction and RV computation methods have been described in Setiawan et al. (2003). From our long-term RV surveys (2003 to 2010) with FEROS, an accuracy in RV of  $11 \text{ m s}^{-1}$  has been measured for a spectroscopic RV standard star HD 10700 (spectral type K8V).

However, this accuracy cannot be achieved for stars with fewer absorption lines due to higher effective temperature and for fast rotating stars, since the spectral lines are broader. We obtained a typical accuracy of  $\sim 50 \text{ m s}^{-1}$  for the individual RV measurements of HIP 13044. In total, 37 high-resolution stellar spectra have been obtained with FEROS. However, one spectrum could not be used for the RV analysis due to a calibration problem. Thus, we use 36 spectra for our spectroscopic study. For HIP 13044 (spectral type F2) we measured the stellar RVs by computing

the cross-correlations of the stellar spectra with a mask, designed for stars of the spectral type F0. In addition, we also created a special cross-correlation mask from the mean spectrum of HIP 13044 spectra. This mask, called "HIP13044 temp", contains 550 selected spectral lines. To find out if there is inconsistency in the characteristics, such as period and amplitude, of the RV variation, as a result of using two different masks, we cross-correlated the spectra of HIP 13044 with this special mask HIP13044-temp. Except the zero-point offsets, we found no discrepancies in the period and amplitude of the RV variation when using either the F0 or the HIP13044-temp masks. Thus, in this work we present only the RV measurements with the standard F0 mask.

The RV values of HIP 13044 have been computed from the mean RVs of 20 usable echelle orders. Table S2 gives the values of the RV measurements. A periodogram analysis by using a Lomb-Scargle (LS) periodogram (Scargle 1982) shows a significant peak at  $P \sim 16$  days with a False Alarm Probability ( $FAP_{LS}$ ) of  $2 \times 10^{-3}$ . In addition, we also applied the Generalized Lomb-Scargle (GLS) periodogram (Zechmeister & Kürster 2009) on the data. By using GLS we found the highest peak at  $P = 16.23$  days with a  $FAP_{GLS} = 5.5 \times 10^{-6}$  (Fig. 4). The RV variation has a semi-amplitude of  $120 \text{ m s}^{-1}$ .

### 2.3. Stellar activity

Stellar activity is an important issue when interpreting the observed RV variations. Stellar rotational modulation is particularly critical when probing the planetary hypothesis. It can mimic the star's reflex motion from a companion and so lead to a wrong interpretation of the RV variation. Another type of stellar activity that can produce periodic RV variation is stellar pulsation. We investigate both types of stellar activity of HIP 13044 in the following subsections.

### 2.3.1. Rotational modulation

A first approximation of the stellar rotation period can be obtained from the knowledge of the projected rotational velocity  $v \sin i$  and stellar radius  $R_*$ . The maximum rotation period can be calculated from  $P_{\text{rot}}/\sin i = 2\pi R_*/v \sin i$  where  $i$  is the inclination angle of the stellar rotation axis. With a stellar radius of  $6.7 R_\odot$  and  $v \sin i = 10.25 \text{ km s}^{-1}$ , we obtained a maximum rotation period of  $\sim 33$  days. However, since  $\sin i$  remains unknown, the real rotational period cannot be determined by this method. Obviously, a better approach should be made to determine the rotation period of the star. Photometric observation is a known classical method to find stellar rotational modulation. Periodic photometric variation due to migrating surface inhomogeneities (starspots) can reveal the stellar rotation. However, although there are photometric observations by Hipparcos and SuperWASP of HIP 13044, the observed variations, even if they are periodic, still cannot be directly interpreted as the result of the stellar rotational modulation. For post main-sequence stars like RGB and HB stars, short-period variations of hours to few days in the photometry are usually caused by the stellar pulsations rather than by rotational modulation.

### *Bisector*

We investigated the rotational modulation by examining the variation of the line profile asymmetry (bisector). In this work we use the bisector velocity span (BVS) which gives the velocity difference between the upper and lower part of the absorption line profile (for a definition of BVS see e.g. Hatzes 1996). We examined the BVS of the stellar spectra and searched for evidence for correlation between BVS and RV variation. As shown in Fig. 5 we found only a weak correlation between BVS and RV (correlation coefficient  $c = -0.13$ ). Since the correlation coefficient is sensitive to the potential outliers in the data, we have carefully investigated this factor by removing few “outliers” in Fig. 5. The highest correlation coefficient we obtained after removing 4 outliers

is  $c = -0.4$ . By bootstrapping the data 100,000 times, we derived a standard deviation of 0.16 for  $c$ . Together with the original value ( $c = -0.13$ ), this confirms the weakness of the correlation between BVS and RV.

Interestingly, we found that the BVS variation shows a clear periodicity of 5.02 days. The  $FAP_{GLS}$  of this period is  $1.4 \times 10^{-5}$ . Fig. 6 shows the periodogram of BVS and the phase-folded BVS variation. Following the idea that migrating starspots on the stellar surface cause the variations in the line profile asymmetry or BVS, which is an effect of the rotational modulation, the period of  $P_{BVS} = 5.02$  days is a possible candidate for the stellar rotation period. In particular, we found no period around 16 days in the BVS variation. Hence, for HIP 13044 the period of the RV variation can be distinguished clearly from the anticipated stellar rotation period.

#### *Ca II $\lambda 8498$ equivalent width*

The emission cores in Ca II K ( $\lambda 393.4$ ) and H ( $\lambda 396.7$ ) as well as the Ca II IR triplet lines ( $\lambda 849.8, 854.2, 866.2$ ) are well known stellar activity indicators. However, for HIP 13044 we found no periodic variation of the Ca II K lines. We did not use the Ca II H line for our analysis since it is blended by the H  $\epsilon$  line.

Furthermore, we measured the equivalent width (EW) of Ca II IR triplets. While we did not find any periodicities in Ca II  $\lambda 854.2$  and  $\lambda 866.2$ , we found periodic EW variations in Ca II  $\lambda 849.8$ . The LS periodogram shows a peak at 5.78 days with a marginal  $FAP_{LS}$  of  $\sim 4\%$  (Fig. 7), whereas the GLS periodogram shows a period of 6.31 days ( $FAP_{GLS} = 4.4 \times 10^{-6}$ ), as shown in Fig. 8. The small discrepancy between the two periods could result from the different fitting and weighting methods used in both periodograms. We conclude that the activity indicator Ca II 849.8 has a period of  $6.05 \pm 0.3$  days.

The results from BVS and Ca II  $\lambda 8498$  EW variation lead to the conclusion that the stellar

rotation period lies between 5 and 6 days. Finally, we adopted  $P = 5.53 \pm 0.73$  days, i.e., the mean value of the periods of both spectroscopic activity indicators as the rotation period of HIP 13044.

### 2.3.2. *Stellar pulsations*

#### *Pulsations of Horizontal Branch stars*

Radial and non-radial stellar pulsations have been observed in post main-sequence stars, such as RGB, AGB stars and white dwarfs. Indeed, many HB stars are also known to be pulsators. However, until now there are not many studies or reported detections of RHB stellar pulsations. Theoretical models of pulsations of red variable HB stars by Xiong et al. (1998) predicted that the oscillation periods of high-order overtones are of the order of a few tenths of a day (few hours).

Furthermore, the oscillation frequency  $\nu_{\max}$  can be predicted from an empirical relation by Kjeldsen & Bedding (1995). For HIP 13044 we calculated  $\nu_{\max} \approx 53 \mu\text{Hz}$  which corresponds to a pulsation period of  $\sim 5.2$  hours. This hypothesis has some support from the studies of HB stars in metal-poor globular clusters, e.g., NGC 6397 (Stello & Gilliland 2009).

#### *RR Lyrae variables*

Since the location of HIP 13044 in the Horizontal Branch is close to the RR Lyrae instability regime, it is also important to investigate the pulsations of those stars and compare them to the detected RV periodicity in HIP 13044. Hartman et al. (2009) observed photometric variability in the metal-poor cluster M3. They found 180 variable stars with periods within 1 day. Similar observations, but for M15 by Corwin et al. (2008) showed that the RR Lyrae variables in M15 have pulsation periods between 0.06 and 1.44 days. These results show that a period of  $\sim 16$  days

is not likely for oscillation characteristics of RR Lyrae stars.

### *W Virginis variables*

W Virginis variable stars belong to Population II Cepheids that have pulsation periods of 10 to 30 days. Thus, there might be a concern about the  $\sim 16$  day periodicity in HIP 13044 being due to pulsations rather than a planetary companion. However, this requires that HIP 13044 itself must belong to W Virginis variables.

Since for W Virginis stars, similar to the classical Cepheids there exist Period-Luminosity relations (e.g. Cox 1979), one can calculate the expected stellar luminosity from the oscillation period. Wallerstein & Cox (1984) listed some basic data of the Population II Cepheids in globular clusters. For Population II Cepheid stars with periodicities of  $\sim 16$  days in the globular clusters M3, M10, M2 and  $\omega$  Cen, their absolute magnitudes  $M_V$  are between -2.2 and -2.7 mag. This is about 3 magnitudes higher than the absolute magnitude of HIP 13044 ( $M_V \sim 0.6$ ). Less luminous Population II Cepheid stars with  $M_V$  between 0.1 and 0.6 are expected to exhibit pulsations with periods of 1–2 days.

Additionally, according to Pritzl et al. (2003) one can calculate the absolute magnitude of the star, if it indeed belongs to W Virginis variables. For  $P = 16.2$  days, the expected absolute magnitude  $M_V$  is -1.925 mag. Because of the lack of supporting W Virginis characteristics, we concluded that HIP 13044 does not belong to the W Virginis variables. The 16 day periodicity is, therefore, not related to the stellar oscillations.

### *Photometric data*

We analyzed the Hipparcos photometry data to investigate the effect of the stellar pulsations. 168 photometric measurements of HIP 13044 are available in the public archive. The LS periodogram

of the Hipparcos data shows no significant signal. The highest peak corresponds to a period of 7.1 hours with a marginal FAP=1.8%. If this period is true, it would be in agreement with the predicted pulsation frequency (Kjeldsen & Bedding 1995). The Hipparcos data is, however, not sufficient to derive more information about the stellar pulsations.

In addition, we also analyzed the photometric observations taken by the SuperWASP project Pollacco et al. (2006). The observations were carried out in 2 blocks, each of 3–4 months. For HIP 13044 there are 3620 photometric measurements available in the archive. After removing 10 outliers, probably caused by systematic errors, we used 3610 data points for the periodogram analysis. With such a large number of measurements, a possible 16-d periodicity in the photometric variations should be easily detectable.

In Fig. 9 we present the LS-periodogram of the SuperWASP data. The LS-periodogram shows few marginal significant (FAP~1%) intra-day periodicities. However, it is not clear, if these signals can be attributed to the stellar oscillations as predicted by the theory. Interestingly, we observe significant peaks at 3.5 days (FAP= $2 \times 10^{-4}$ ) and 1.4 days (FAP= $5 \times 10^{-4}$ ). The two signals are most likely harmonic to each other. Since the FAPs of both signals are of the same order ( $10^{-4}$ ), the determination of the exact value of the period is still difficult. It is also possible that these periods correspond to oscillation overtones of very high order. Most important, however, is the fact that no signal at 16.2 days is detected in the LS-periodogram of the SuperWASP photometry data. Due to the absence of a periodic photometric variation of 16.2 days, stellar pulsations are not likely to be the source of the observed periodic RV variation.

## 2.4. Concluding remarks

Based on the spectroscopic and photometric analysis described above, stellar rotational modulation and pulsations can be ruled out as the source of the periodic RV variation. The

spectroscopic stellar activity indicators show a period of 5–6 days (bisectors and Ca II  $\lambda 849.8$ ) whereas the photometric data shows periodicities of intra-day to few days, that can be clearly distinguished from the period of the RV variation. We conclude that the observed 16.2 days RV variation cannot be due to rotational modulation or stellar pulsations, but is rather caused by the presence of an unseen planetary companion.

### **Acknowledgements**

We thank our MPIA colleagues: W. Wang, C. Brasseur, R. Lachaume, M. Zechmeister and D. Fedele for the spectroscopic observations with FEROS. We also thank Dr. M. Perryman, Dr. E. Bear, Dr. N. Soker and Dr. P. Maxted for the fruitful discussion, comments and suggestions that helped to improve this paper.

Table. S2

RV measurements of HIP 13044

<b>Julian Date</b>	<b>RV</b>	$\sigma$	<b>Julian Date</b>	<b>RV</b>	$\sigma$
-2450000	-300 km/s	m/s	-2450000	-300 km/s	m/s
5103.8853	4225.32	50.50	5225.6069	4288.14	58.04
5106.7933	4258.74	47.50	5254.5296	4003.23	56.92
5164.7565	4282.91	50.86	5255.5402	4097.93	52.17
5168.6543	4169.13	50.22	5256.5457	4178.24	46.06
5170.7212	4102.30	50.42	5258.5407	4240.39	56.84
5172.6968	4081.84	63.61	5262.5523	4279.91	55.03
5174.6528	4062.56	42.69	5263.5499	4276.28	52.83
5175.5576	4116.08	51.69	5268.5164	4066.90	48.92
5197.5703	4282.29	47.90	5269.5159	4101.27	69.23
5199.5236	4285.80	48.63	5396.8722	4240.15	53.09
5199.5666	4264.87	44.12	5397.8666	4196.54	75.11
5200.6345	4223.49	51.08	5399.8604	4089.90	111.8
5202.6003	4094.38	46.72	5400.9307	4006.32	52.99
5203.6050	4017.79	54.59	5401.8926	4095.39	53.14
5204.6531	4148.22	64.52	5402.8419	4081.08	113.26
5223.6119	4017.52	54.59	5403.8388	4153.56	85.38
5224.5837	4203.70	51.66	5404.8850	4232.36	57.91
5225.5329	4180.37	50.41	5405.8472	4249.60	78.77

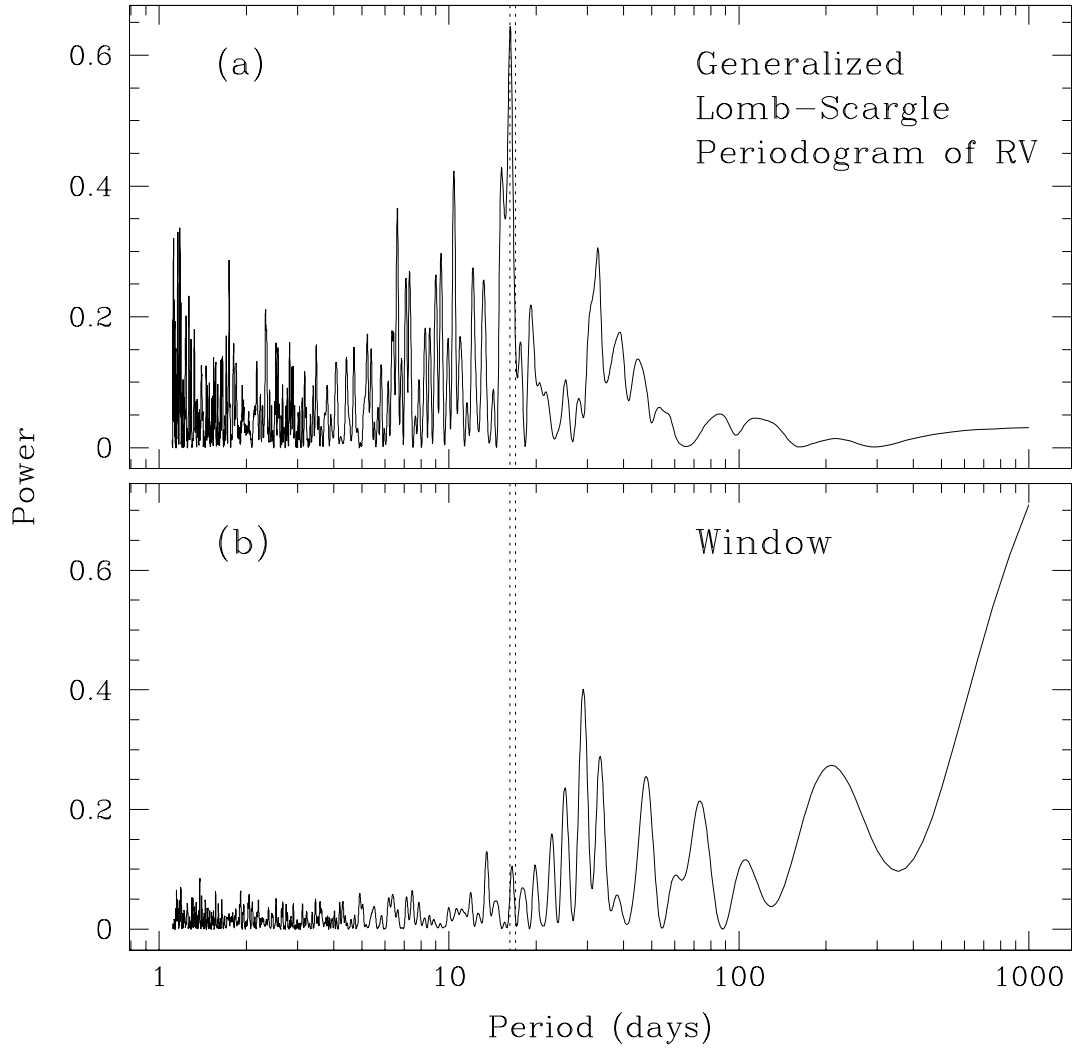


Fig. 4.— Upper panel: Generalized Lomb-Scargle (GLS) Periodogram of the RV measurements of HIP 13044. The window function is shown in the lower panel. The GLS periodogram shows a significant peak at  $\sim 16$  days (dotted lines). The window function does not show any peak around this period.

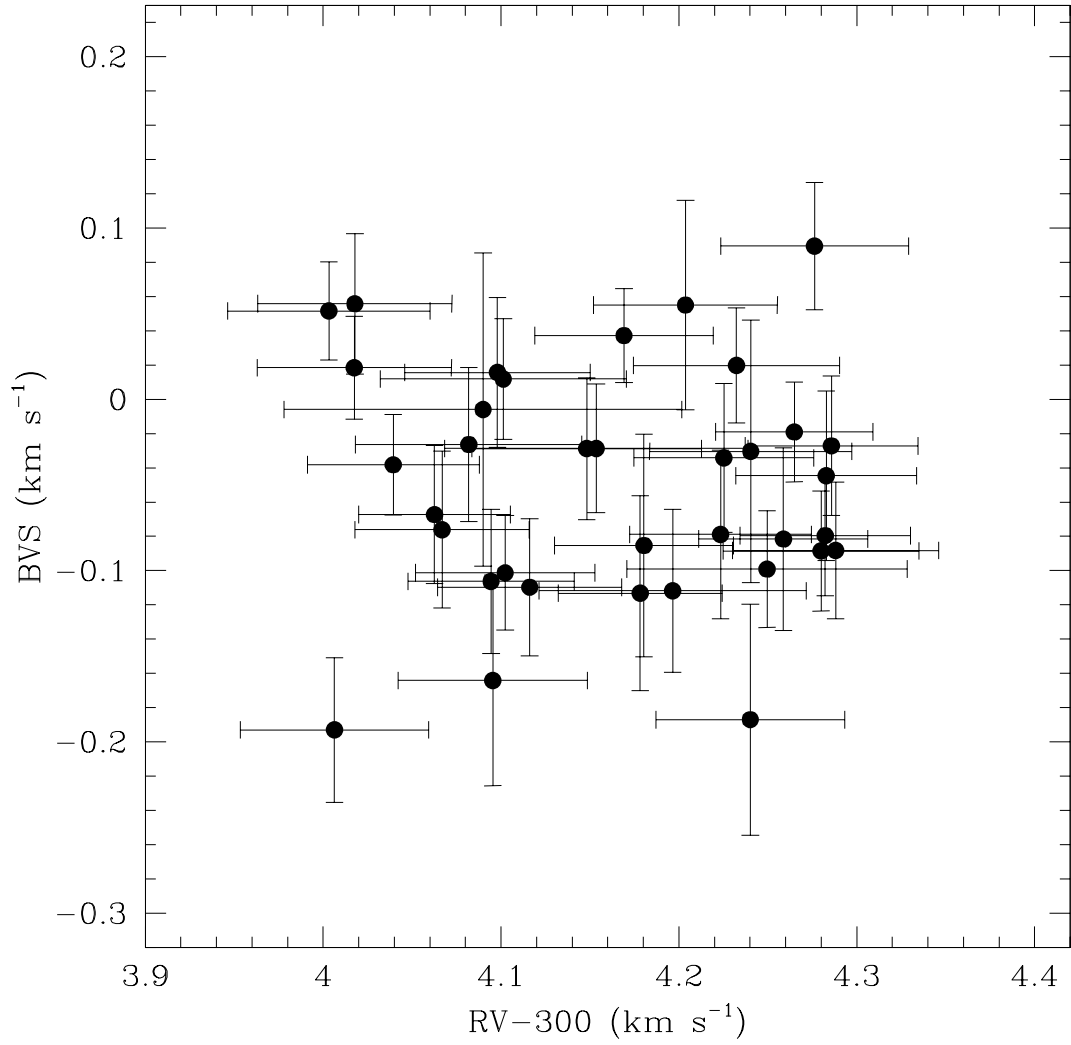


Fig. 5.— The plot of BVS versus RV shows a weak correlation between both quantities. With all 36 points we calculated a correlation coefficient of -0.13. A careful rejection of 4 potential "outliers" yields a correlation coefficient of -0.4, which is slightly higher, but still insignificant.

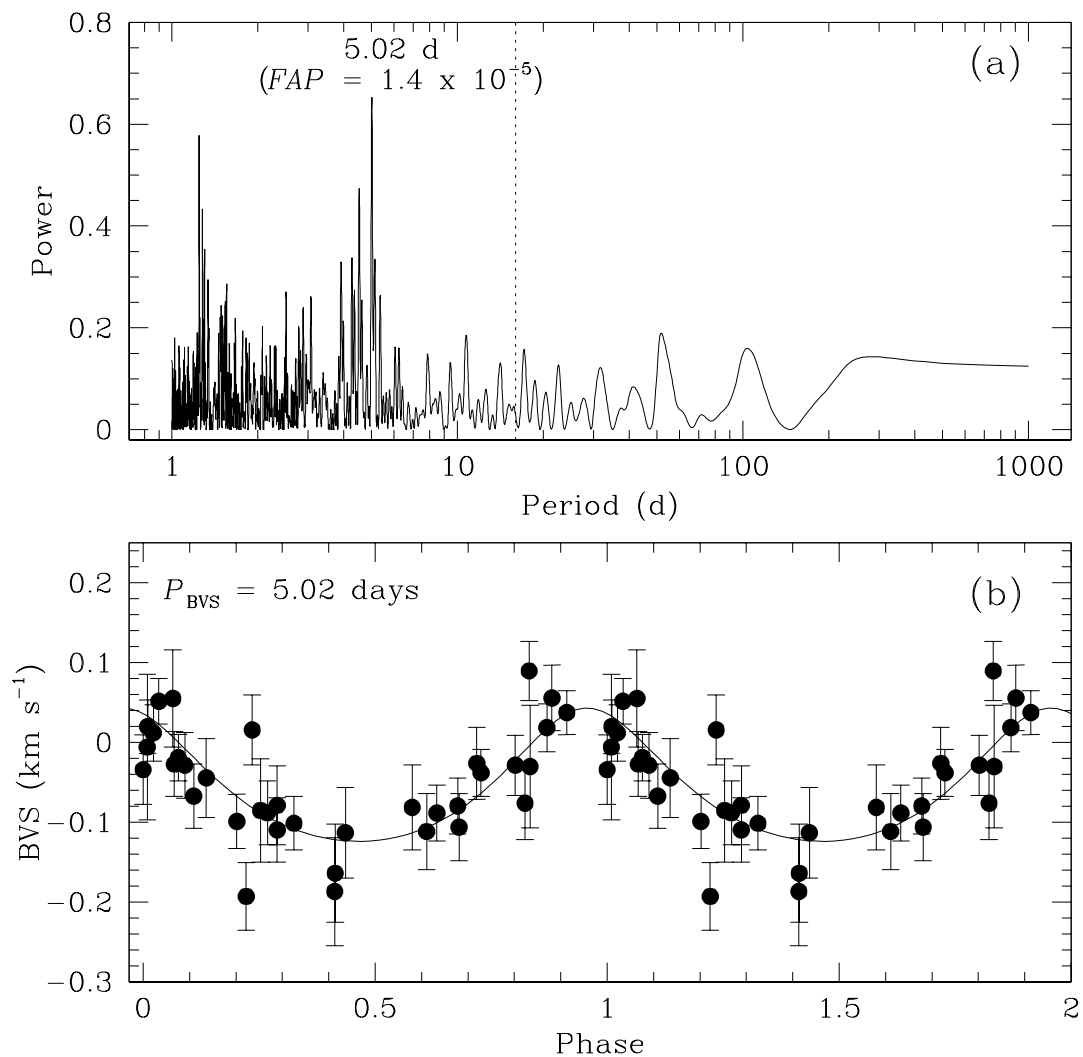


Fig. 6.— Periodogram analysis of the BVS variation showing a periodicity of 5.02 days with a FAP of  $1.4 \times 10^{-5}$  (upper panel). The lower panel shows a phase-folded plot of the BVS variation. The semi-amplitude of the variation is  $\sim 70\text{m s}^{-1}$ .

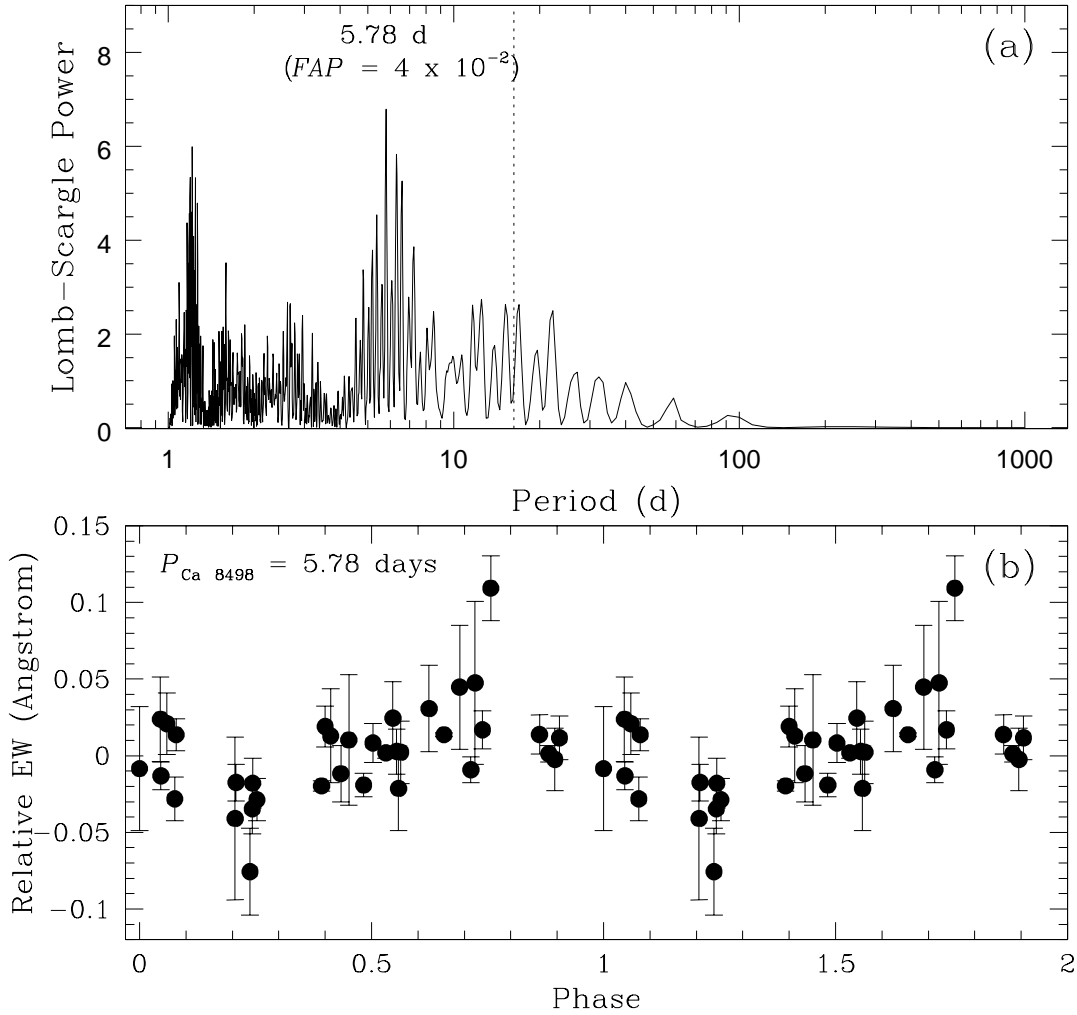


Fig. 7.— Analysis of the CaII  $\lambda 849.8$  EW variation by using a Lomb-Scargle periodogram. The LS-periodogram shows a peak at 5.78 days with a marginal FAP of 4%. The lower panel is the plot of the EW variation of CaII  $\lambda 849.8$  that is phase-folded with a period of 5.78 days.

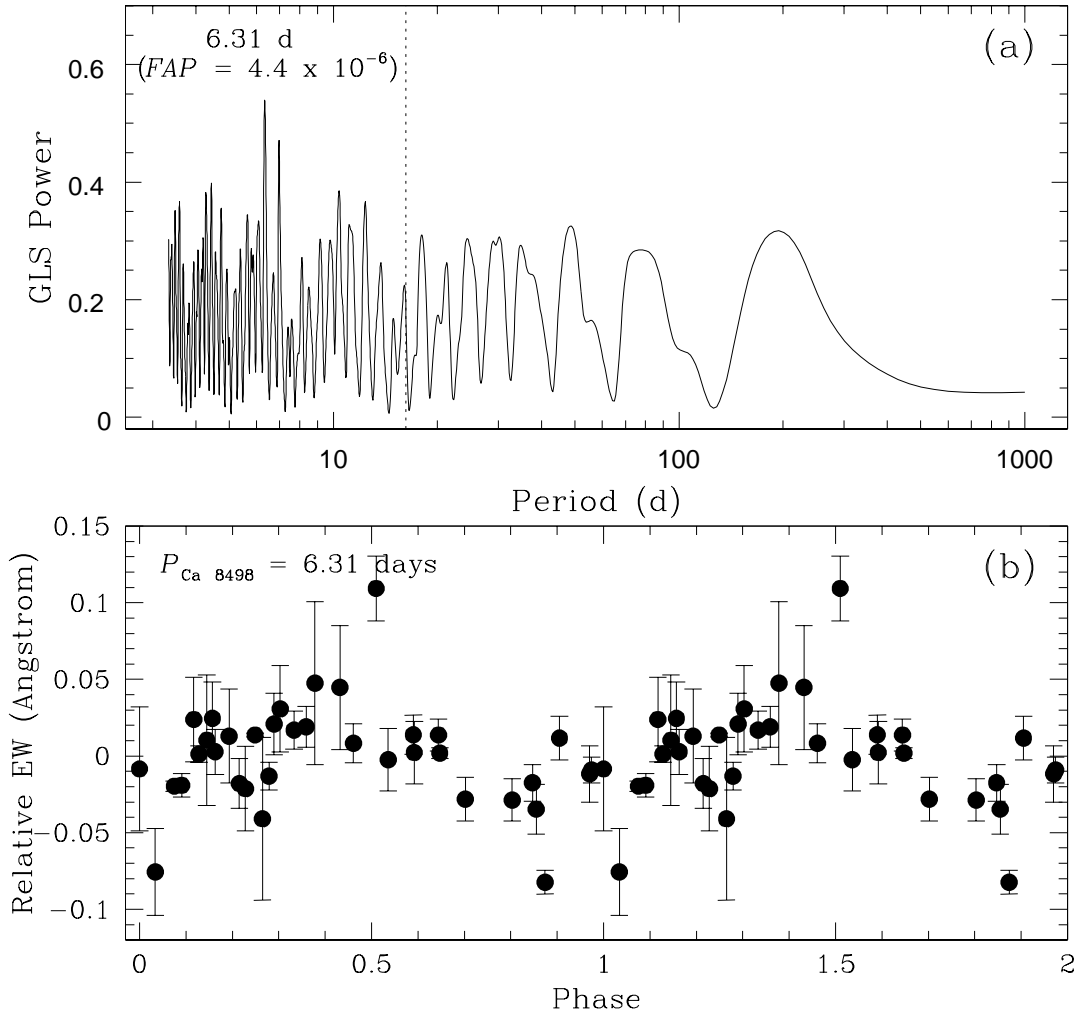


Fig. 8.— Analysis of the CaII  $\lambda 849.8$  EW variation by using the Generalized Lomb-Scargle periodogram. The period found in the GLS-periodogram is only slightly different from that obtained from the LS-periodogram. The GLS-periodogram shows a peak at 6.31 days with a FAP of  $4.4 \times 10^{-6}$ . The phase-folded plot with  $P = 6.31$  days is shown in the lower panel.

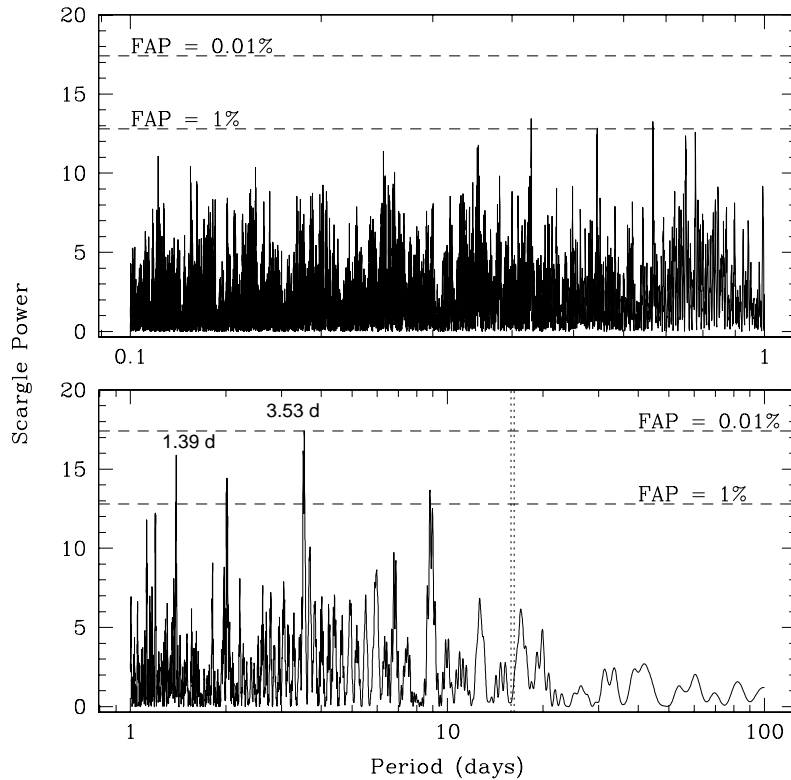


Fig. 9.— Lomb-Scargle periodogram of the SuperWASP photometry data. The periodogram shows only marginal significant ( $FAP \sim 1\%$ ) peaks that correspond to intra-day periodicities (upper panel). It is not clear, if these signals are related to the stellar oscillations predicted by the theory. Nevertheless, in the lower panel the periodogram shows two significant peaks at 3.53 days ( $FAP = 2 \times 10^{-4}$ ) and 1.39 days ( $FAP = 5 \times 10^{-4}$ ). These signals are probably harmonic to each other. In this extensive data set no photometric variation with a period of  $\sim 16$  days has been detected (dotted lines).

## REFERENCES

- Bear, E., & Soker, N., 2010, *ArXiv e-prints 1003.4884*
- Beer, M. E., King, A. R., & Pringle, J. E., 2004, *MNRAS*, 355, 1244
- Beers, T. C., Preston, G. W., Shectman, S. A., & Kage, J. A., 1990, *AJ*, 92, 60
- Buonanno, R., Corsi, C. E., Buzzoni, A., Cacciari, C., Ferraro, F. R., & Fusi Pecci, F., 1994, *A&A*, 290, 69
- Carlberg, J. K., Majewski, S. R., & Arras, P., 2009, *ApJ*, 700, 832
- Carney, B. W., & Latham, D. W., 1986, *AJ*, 125, 293
- Carney, B. W., Latham, D. W., Stefanik, R. P., Laird, J. B., & Morse, J. A., 2003, *AJ*, 125, 293
- Carney, B. W., Latham, D. W., Stefanik, R. P., & Laird, J. B., 2008, *AJ*, 135, 196
- Carney, B. W., Gray, D. F., Yong, D., Latham, D. W., Manset, N. et al. (7 authors), 2008, *AJ*, 135, 892
- Chiba, M., & Beers, T.C., 2000, *AJ*, 119, 2843
- Corwin, T. Michael, Borissova, J., Stetson, Peter B., et al. (4 authors), 2008, *AJ*, 135, 1459
- Cox, A. N., 1979, *ApJ*, 229, 212
- Döllinger, M. P., Hatzes, A. P., Pasquini, L., Guenther, E. W., Hartmann, M., Girardi, L., & Esposito, M., 2007, *A&A*, 472, 649
- Ford, E. B., Joshi, K. J., Rasio, F. A., & Zbarsky, B., 2000, *ApJ*, 528, 336
- Geier, S., Edelmann, H., Heber, U., & Morales-Rueda, L., 2009, *ApJ*, 702, L96

Gonzalez, G., 1997, MNRAS, 285, 403

Gray, D. F., Carney, B. W., & Yong, D., 2008, AJ, 135, 2033

Gregory, P. C., 2005, *Bayesian Logical Data Analysis for the Physical Sciences: A Comparative Approach with 'Mathematica' Support*, Cambridge University Press

Harris, W. E., 1996, AJ, 112, 1487

Hartman, J. D., Kaluzny, J., Szentgyorgyi, A., Stanek, K. Z., 2005, AJ, 129, 1596

Hatzes, A. P., & Cochran, W. D., 1993, ApJ, 413, 339

Hatzes, A. P., 1996, PASP, 108, 839

Helmi, A., White, S. D. M., de Zeeuw, P. T., Zhao, H., 1999, Nature, 402, 53

Heyl, J., 2007, MNRAS, 382, 915

Ida, S., & Lin, D. N. C., 2005, *Progress of Theoretical Physics Supplement*, 158, 68

Johnson, J. A., Howard, A. W., Bowler, B. P., Henry, G. W., Marcy, G. W., Wright, J. T., Fischer, D. A., & Isaacson, H., 2010, PASP, 122, 701

Kaufer, A., Stahl, O., Tubbesing, S. et al., 2000, SPIE, 4008, 459

Kepley, A. A., Morrison, H. L., Helmi, A., Kinman, T. D., van Duyne, J., et al. (7 authors), 2007, AJ, 134, 1579

Kjeldsen, H. & Bedding, T. R., 1995, A&A, 293, 87

Klement, R., Rix, H. W., Flynn, C., Fuchs, B., Beers, T. C. et al., 2009, ApJ, 698, 865

Lee, J. W., Kim, S.-L., Kim, C.-H., Koch, R. H., Lee, C.-U., Kim, H.-I., & Park, J.-H., 2009, AJ, 137, 3181

- Levrard, B., Winisdoerffer, C., & Chabrier, G., 2009, *ApJ*, 692, L9
- Livio, M., & Soker, N., 1983, *A&A*, 125, L12
- Mathis, J. S., & Lamers, H. J. G. L. M., 1992, *A&A*, 259, L39
- Maxted, P. f. L., Heber, U., Marsh, T. R., & North, R. C., 2001, *MNRAS*, 326, 1391
- Perryman, M. A. C., Lindegren, L., Kovalevsky, J. et al., 1997, *A&A*, 323, 49
- Pollacco, D. L., Skillen, I., Cameron, A. Collier et al. (25 authors), 2006, *PASP*, 118, 1407
- Pritzl B. J., Smith Horace A., Stetson, Peter B., et al. (4 authors), 2003, *AJ*, 126, 1381
- Roederer, I. U., Sneden, C., Thompson, I. B., Preston, G. W., & Shectman, S. A., 2010, *ApJ*, 711, 573
- Santos, N. C., Israelian, G., & Mayor, M., 2004, *A&A*, 415, 1153
- Scargle, J. D., 1982, *ApJ*, 263, 835
- Setiawan J., Pasquini, L., da Silva, L., von der Lühe, O., Hatzes, A. P., 2003, *A&A*, 397, 1151
- Setiawan J., Pasquini, L., da Silva, L. et al. (5 authors), 2004, *A&A*, 421, 241
- Shkolnik, E., Bohlender, D. A., Walker, G. A. H., & Collier Cameron, A., 2008, *ApJ*, 676, 628
- Sigurdsson, S., Richer, H. B., Hansen, B. M., Stairs, I. H., Thorsett, S. E., 2003, *Science*, 301, 193
- Silvotti, R., Schuh, S., Janulis, R., et al. (20 authors), 2007, *Nature*, 449, 189
- Simon, N. R., 1992, *ApJ*, 387, 162
- Soker, N., 1998, *AJ*, 116, 1308

Sozzetti, A., Torres, G., Latham, D. W., Stefanik, R. P., Korzennik, S. G., Boss, A. P., Carney, B. W., & Laird, J. B., 2009, *ApJ*, 697, 544

Stello, D. & Gilliland, R. L., 2009, *ApJ*, 700, 949

Valenti, J. A., & Fischer, D. A., 2005, *ApJS*, 159, 141

Wallerstein, G. & Cox, A. N., 1984, *PASP*, 96, 677

Walker, G. A. H., Bohlender, D. A., Walker, A. R., Irwin, A. W., Yang, S. L. S., & Larson, A., 1992, *ApJ*, 396, L91

Xiong, D. R., Cheng, Q. L., Deng, L., 1998, *ApJ*, 500, 449

Zechmeister, M., & Kürster, M., 2009, *A&A*, 496, 577